

Influence of polytypism on thermal properties of silicon carbide

A. Zywietz, K. Karch, and F. Bechstedt

Friedrich-Schiller-Universität, Institut für Festkörpertheorie und Theoretische Optik, Max-Wien-Platz 1, 07743 Jena, Germany

(Received 6 December 1995; revised manuscript received 29 February 1996)

We present calculations of thermal properties of the $3C$, $6H$, $4H$, and $2H$ polytypes of silicon carbide (SiC). The underlying lattice-dynamical properties are calculated within a generalized bond-charge model which gives also correct phonon eigenvectors. In the case of the zinc-blende structure the results are checked by comparison with those of *ab initio* density-functional calculations. Explicitly, we determine the free energy, the specific heat, the Debye temperature, and the Debye-Waller factors. The influence of the polytypism, in particular of the anisotropy in the hexagonal cases, is studied in detail. The theoretical results are in good agreement with available experimental data. A temperature-dependent axial next-nearest-neighbor Ising model is derived. Consequences are discussed for the polytypism and the thermodynamics of the different SiC phases. [S0163-1829(96)11627-1]

I. INTRODUCTION

The growing interest in the semiconductor silicon carbide (SiC) is related to applicative and scientific reasons. SiC is an attractive material for electronic devices in high-temperature and high-power applications because of its large band gap, large thermal conductivity, high breakdown voltage, and of its outstanding mechanical and chemical stability. SiC, which is the only known naturally stable group-IV compound, exhibits a very pronounced polytypism. More than 200 crystalline modifications have been determined to date.¹ Zinc-blende ($3C$) SiC, with pure cubic stacking of Si-C double layers in the $[111]$ direction, and wurtzite ($2H$) SiC, with pure hexagonal stacking in $[0001]$ direction, are the most extreme polytypes. The other polytypes represent hexagonal (H) and rhombohedral (R) combinations of these stacking sequences with n Si-C bilayers in the primitive cell.² The polytypes lie very close together in energy and possess similar lattice constants.³⁻⁵ For example, the most common polytypes $3C$, $6H$, $4H$, and $2H$ differ only by about 0.1% in the lattice constant a . The indirect band gap varies between 2.4 eV ($3C$) and 3.3 eV ($2H$).⁶ On the other hand, the lattice-dynamical properties are rather similar.⁷ Apart from the folding of the phonon modes the strongest effect is related to the anisotropy of the long-range electric field accompanying the excitation of polar optical phonons. The Γ point phonon frequencies vary within an interval of 5 cm^{-1} versus the polytypes. However, a remarkable redistribution in the density of states of the optical phonon modes has been found.⁷

The knowledge of the temperature dependence of physical quantities is important for many equilibrium properties. This holds especially for the Helmholtz free energy, which governs the whole thermodynamics. Important information about the polytypism of the material system as well as the growth conditions of the various polytypes may be derived within the harmonic approximation, even if the relevance of an equilibrium theory is restricted to low temperatures.⁸ The displacement-displacement correlation functions describe the temperature-dependent motion of the ions in the crystal. They also determine the Debye-Waller factors and, hence,

the temperature dependence of spot intensities in many diffraction spectroscopies, such as x-ray diffraction or neutron scattering. The heat capacity, in particular for low temperatures where it may be directly related to the Debye temperature, characterizes the dynamical and thermal properties of the crystal in an averaged manner.

In this paper we present calculations of thermal properties of $3C$, $6H$, $4H$, and $2H$ SiC polytypes using a generalized bond charge model to describe the lattice dynamics.⁷ Our computations include thermodynamic functions, i.e., free energy and entropy, heat capacity, and autocorrelation (mean square displacements) of atomic displacements. We study the influence of the polytypism on these quantities, in particular the influence of hexagonality and anisotropy. Moreover, we discuss the thermodynamical stability of the polytypes. For that purpose a linear Ising spin (ANNNI) model with temperature-dependent parameters is introduced. Comparison with experimental data is performed for the specific heat at constant volume and the Debye-Waller factors. In the case of $3C$ SiC the quality of the bond-charge-model results is directly checked by comparing with first-principles density functional calculations.^{9,10}

II. CALCULATIONAL METHOD

A generalization of the adiabatic bond-charge model (BCM) is used to calculate the phonon frequencies $\omega_j(\mathbf{q})$ as well as the corresponding eigenvectors $\mathbf{e}^K(j\mathbf{q})$ within the harmonic approximation.⁷ The BC model contains 10 (16) free parameters for the cubic (hexagonal) case. These parameters have been fitted to reproduce the first-order Raman frequencies. In the BC model, an atom is described by a charged ion, whereas the bonds are replaced by massless bond charges. These charges interact via central and angular forces up to second-nearest neighbors. The BC model is chosen, since it describes reasonably not only the phonon frequencies but also the phonon eigenvectors as shown in Ref. 7. As shown in Refs. 9–13 the anharmonic corrections up to the second order in the cubic and first order in the quartic anharmonic coupling constants for homopolar and heteropolar semiconductors are rather small for thermal properties

like free energy and entropy or specific heat at constant volume up to the temperature $1/2T^*$, whereby the temperature $T^* = \hbar \omega_{\max}/k_B$ corresponds to the maximum frequency of the phonon spectrum. Therefore, for temperatures below 700 K the anharmonic contributions to the thermal properties of SiC considered here can be safely neglected. The thermal properties for which anharmonic contributions at every temperature are not negligible, such as the linear expansion coefficient or the difference of the specific heat at constant volume and constant pressure, are not considered here. The correct description of the phonon eigenvectors is crucial for the investigation of the displacement-displacement correlations of atoms. The correlation of atomic displacements $\mathbf{u}(\kappa l)$ and $\mathbf{u}(\kappa' l')$ is defined as

$$\langle u_\alpha(\kappa l) u_\beta(\kappa' l') \rangle = \frac{\hbar}{\sqrt{M_\kappa M_{\kappa'}}} \frac{1}{N} \sum_{\mathbf{q}, j} \frac{1}{\omega_j(\mathbf{q})} \left[n(\omega_j(\mathbf{q})) + \frac{1}{2} \right] \times e^{i\kappa \cdot \mathbf{R}_j} e^{i\kappa' \cdot \mathbf{R}_j} e^{i\mathbf{q} \cdot (\mathbf{R}_l - \mathbf{R}_{l'})}, \quad (1)$$

where M_κ is the atomic mass of the κ th atom, \mathbf{R}_j is a Bravais lattice vector, $n(\omega) = [\exp(\hbar\omega/k_B T) - 1]^{-1}$ is the average phonon occupation number (Bose function), and N denotes the number of unit cells in the crystal.

Whereas in the case of 3C SiC ($F\bar{4}3m$ space group symmetry) all atomic positions are fixed by the cubic lattice constant a , the knowledge of the lattice constants a and c as well as of $n/2$ internal free parameters is necessary to fix the atomic position in the case of hexagonal nH polytypes ($P6_3mc$ space group symmetry). However, the atomic relaxations from their ideal positions in nH SiC polytypes are very small.⁴ Moreover, their influence on the lattice dynamical and dielectric properties is negligible.¹⁴ Therefore, we neglect these relaxations and fix the equilibrium atomic positions by experimental values of a and c taken from Ref. 15.

The free energy of any polytype is described by

$$F(T, V) = F_{\text{el}}(T, V) + F_{\text{vib}}(T, V), \quad (2)$$

$$F_{\text{vib}}(T, V) = \sum_{\mathbf{q}, j} \left\{ \frac{1}{2} \hbar \omega_j(\mathbf{q}) + k_B T \ln [1 - \exp(-\hbar \omega_j(\mathbf{q})/k_B T)] \right\}. \quad (3)$$

In our calculations, we replace the electronic contribution $F_{\text{el}}(T, V)$ by its static limit, i.e., the corresponding internal energy of the valence electrons of the system,^{4,5} since the electronic entropy is negligibly small in the interesting temperature range. The lattice contribution is described by the sum over a set of independent harmonic oscillators with frequencies $\omega_j(\mathbf{q})$. The entropy of the vibrating lattice follows from the free energy as $S_{\text{vib}} = -(\partial F_{\text{vib}}/\partial T)_V$. Its knowledge allows the calculation of the internal energy according to $U_{\text{vib}} = F_{\text{vib}} + TS_{\text{vib}}$. Apart from extremely low temperatures, the internal energy of the lattice also defines the heat capacity at constant volume of the crystal by $C_V(T) = (\partial U_{\text{vib}}/\partial T)_V$. From Eq. (3) one obtains for the heat capacity

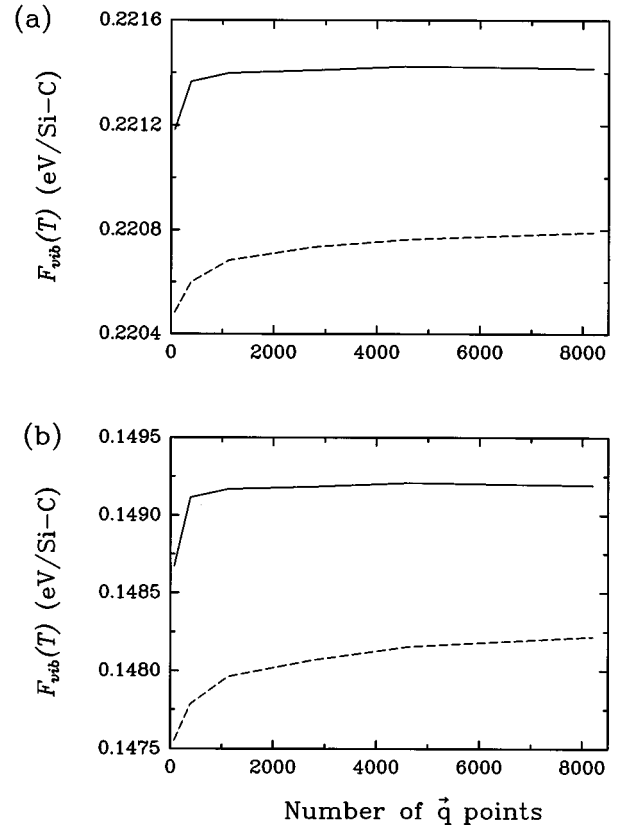


FIG. 1. Convergence of the lattice contribution to the free energy per SiC pair with respect to the number of \mathbf{q} points in the irreducible part of the Brillouin zone for 3C (solid line) and 2H SiC (dashed line) at $T=0$ K (a) and $T=500$ K (b).

$$C_V(T) = \sum_{\mathbf{q}, j} k_B \left(\frac{\hbar \omega_j(\mathbf{q})}{k_B T} \right)^2 \frac{\exp(\hbar \omega_j(\mathbf{q})/k_B T)}{[\exp(\hbar \omega_j(\mathbf{q})/k_B T) - 1]^2}. \quad (4)$$

A dense \mathbf{q} -point sampling is crucial to achieving the desired accuracy in the energy differences. The special-point technique of Monkhorst-Pack is used to perform the integration over the irreducible part of the Brillouin zone (BZ).¹⁶ Because the energy differences between the polytypes are rather small, we sample exactly the same \mathbf{q} -points in the \mathbf{q} -space of all the structures. Therefore, the zinc-blende structure is specified in terms of the hexagonal unit cell (3H). We choose the same mesh of \mathbf{q} -points (34×34) in the plane of hexagonal layers for all structures but different numbers of \mathbf{q} -point layers along the stacking direction; 24, 16, 12, and 8 layers for the 2H, 3H, 4H, and 6H structure, respectively. This choice corresponds to 4624 special points for the 2H structure. The convergence of the free energy of the cubic 3C and the wurtzite 2H structure with respect to the \mathbf{q} -point sampling is shown in Fig. 1. Whereas the differences of the free energy between the SiC structures are of the order of 0.1 meV, the errors in the energy differences using these finite \mathbf{q} -point sets are estimated to be about 0.01 meV per Si-C pair. A dense mesh of special points is in particular decisive for the calculations of the correlation functions. At low temperatures the correlation functions are proportional to the inverse eigenfrequencies, in the high-temperature limit even to the square of the inverse eigenfrequencies. Because

of the linear \mathbf{q} -dependence of the acoustic-mode frequencies, a formal singularity appears at the Γ point [see Eq. (1)]. However, transforming the \mathbf{q} -sum into an integral over the BZ, it becomes evident that this seeming singularity is removed by the \mathbf{q}^2 -dependence of the space element. Nevertheless a rather dense mesh of the special points is needed to obtain well converged results. Therefore, for the calculation of the displacement-displacement correlation functions we have increased the density of the mesh points in the region around the Γ point by a factor 3.

In order to control the results obtained within the BCM, we compare them with those obtained using a first-principles method.^{9,10} In the *ab initio* method the dynamical matrix is derived by calculating the response of the electrons to atomic displacements and static electric fields using density-functional perturbation theory (DFPT). Our calculations are performed within the local-density approximation (LDA) using soft norm-conserving pseudopotentials. The dimension of the plane-wave basis set at a given \mathbf{q} point in the first BZ is fixed by a kinetic-cutoff energy of 40 Ry. This cutoff energy corresponds to about 450 plane waves per atom. Unfortunately, DFPT is computationally very demanding due to the necessity of calculating the electron-density response to a phonon perturbation. Therefore, a calculation of the full phonon spectra cannot be done for polytypes with many atoms in the unit cell, i.e., for 6H SiC. Consequently, we restrict the *ab initio* calculations to the 3C polytype with two atoms in the unit cell.

III. RESULTS

A. Thermodynamics

The thermodynamics of the vibrating crystal lattices is governed by the Helmholtz free energy $F_{\text{vib}}(T, V)$, which depends on the temperature and the volume. The Helmholtz free energy of 3C SiC calculated within the BCM as well as using the DFPT is plotted in Fig. 2(a) versus temperature. In the temperature range considered the discrepancy between the results of both approaches to the harmonic lattice dynamics is rather small. Therefore, we conclude that within the harmonic approximation the BCM is applicable not only to the lattice-dynamical but also to the thermal properties of SiC. The lattice contribution to the total free energy shows the behavior being typical for all crystal lattices. We observe an excellent agreement with a previous calculation,¹⁷ where a valence-overlap shell model was used to describe the phonon frequencies. In the low temperature region, the zero-point vibration of the lattice is the most important contribution to the free energy $F_{\text{vib}}(T, V)$; In this temperature region the free energy is almost independent of temperature, as can be seen in Fig. 2(a). Although the absolute value of the free energy at low temperatures is rather small (0.1%) compared to the static total energy,³⁻⁵ it becomes important for the thermal stability. In the high temperature region the entropy contribution $-TS_{\text{vib}}$ governs the free energy as indicated by the almost linear temperature dependence and the negative free-energy values in this temperature range. The entropy of 3C SiC is plotted in Fig. 3(a). Whereas in the low temperature region the entropy exhibits an exponential increase, the entropy has approximately a logarithmical dependence for higher temperatures.

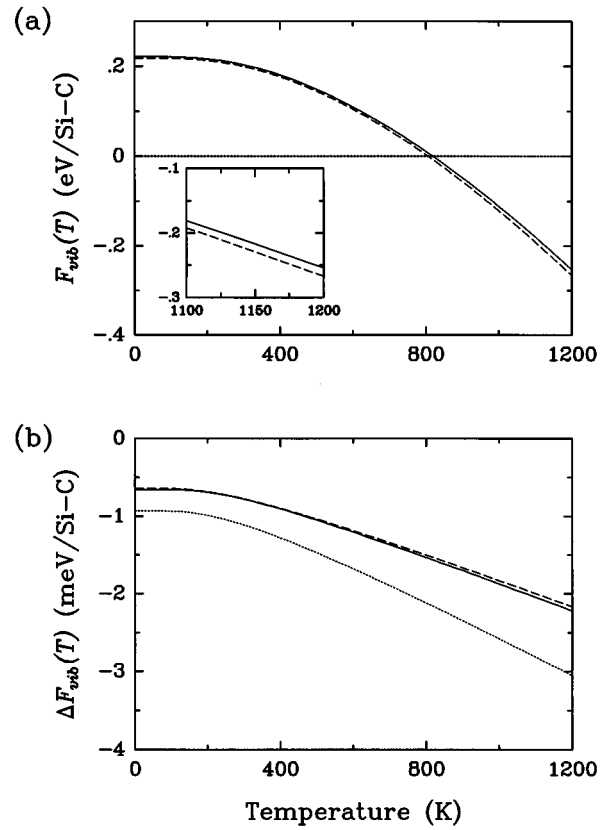


FIG. 2. (a) The calculated free energy of the 3C SiC lattice using a bond-charge model (solid line) and *ab initio* density-functional theory (dashed line). (b) Differences of the free energy of the nH polytypes with respect to the 3C value. $F_{\text{vib}}^{2H} - F_{\text{vib}}^{3C}$ (solid line), $F_{\text{vib}}^{4H} - F_{\text{vib}}^{3C}$ (dotted line), and $F_{\text{vib}}^{6H} - F_{\text{vib}}^{3C}$ (dashed line).

For a discussion of the polytype stabilization by the vibrating lattice only the differences of the lattice contributions to the total energy are substantial. Such differences with respect to the free energy of the zinc-blende structure of SiC are plotted for the hexagonal polytypes 6H, 4H, and 2H with increasing percentage hexagonality h of 33%, 50%, and 100% in Fig. 2(b). Despite the smallness of the absolute values of the lattice contribution to the total free energy per Si-C pair, the differences ΔF_{vib} approach the same order of magnitude, i.e., several meV, as the differences of the static total internal energy.³⁻⁵ In the low temperature region the main contribution is due to the variation of the zero-point vibrational internal energy. For higher temperatures there is also a contribution from the entropy variation [see Fig. 3(b)]. However, the entropy contribution does not change the order of the static energy of the investigated polytypes, but rather enlarges the differences among them. In contrast to the differences in the one-phonon density of states,⁷ we do not observe a clear trend with the percentage hexagonality. In general, the (lattice) free energies are lower for the hexagonal lattices than for the cubic one. We explain this fact by the general tendency that the limiting frequencies slightly decrease with rising hexagonality. This is clearly shown for the zone-center optical phonon frequencies⁷ as well as for the Debye temperature (see discussion below). Such a trend decreases the free energy in the average. On the other hand,

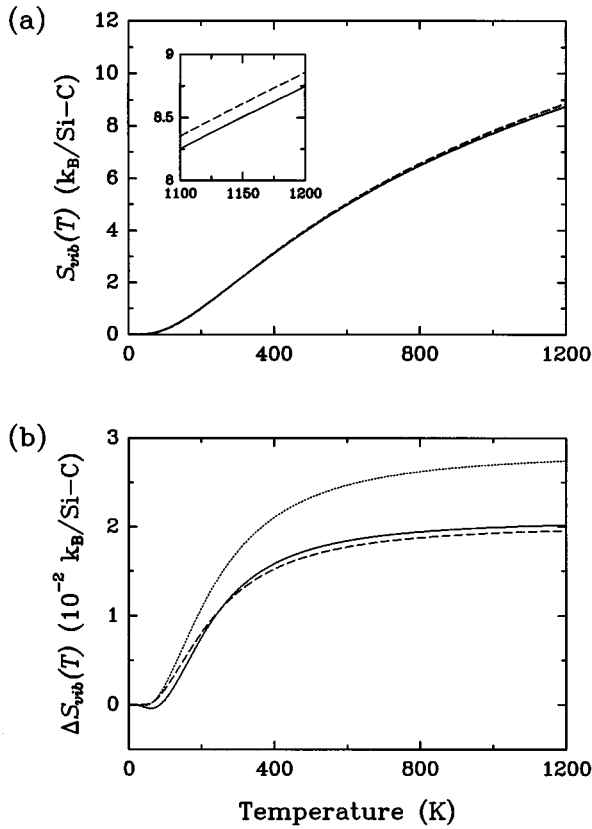


FIG. 3. (a) The entropy of the 3C SiC lattice within the bond-charge model (solid line) and *ab initio* density-functional theory (dashed line). (b) Differences of the entropy of the nH polytypes with respect to the 3C value. $S_{\text{vib}}^{2H} - S_{\text{vib}}^{3C}$ (solid line), $S_{\text{vib}}^{4H} - S_{\text{vib}}^{3C}$ (dotted line), and $S_{\text{vib}}^{6H} - S_{\text{vib}}^{3C}$ (dashed line).

within the hexagonal polytypes 6H, 4H, and 2H there is visible a nearly parabolic dependence of the free energy on the hexagonality, although the variations are smaller than the differences to the 3C values. The lowest free energy is observed for 4H ($h=50\%$), whereas the values for 6H ($h=33\%$) and 2H ($h=100\%$) are nearly identical. Consequently, the vibrating lattice strengthens the tendency for the stabilization of the 4H polytype in the thermodynamic equilibrium. This happens surprisingly not only for low temperatures but also for higher temperatures. Our results for the vibrational contributions to the Helmholtz free energy are somewhat in contrast to those of Cheng *et al.*¹⁷ Cheng *et al.* found differences of the phonon free energies that are one order of magnitude smaller. The reason may be related to the fact that the same valence-overlap shell model parameters derived for cubic SiC are applied to the other hexagonal polytypes. In this manner only differences in the geometrical structure are taken into account but effects related to the long-range electric field, which give rise to the anisotropy of the lattice-dynamical properties and the splittings of the zone center phonon frequencies, are neglected.

B. Temperature-dependent ANNNI model

Geometrically the polytypes differ by the stacking along the cubic [111] or the equivalent hexagonal [0001] direction. Along this particular direction all polytypes may be imag-

TABLE I. Interaction parameters J_i (meV) of the ANNNI model for different temperatures and different electronic contributions to the total free energy taken from Refs. 3–5.

	J_1			J_2			J_3		
Reference	[3]	[4]	[5]	[3]	[4]	[5]	[3]	[4]	[5]
static value	4.80	1.08	2.33	-2.93	-2.45	-3.49	-0.45	-0.18	0.25
0 K	4.49	0.76	2.02	-3.23	-2.75	-3.79	-0.47	-0.19	0.24
400 K	4.38	0.66	1.91	-3.34	-2.86	-3.90	-0.48	-0.21	0.22
800 K	4.10	0.37	1.63	-3.60	-3.13	-4.16	-0.52	-0.24	0.18
1200 K	3.79	0.07	1.32	-3.90	-3.42	-4.46	-0.55	-0.28	0.15

ined as different arrangements of cubic or hexagonal Si-C bilayers.⁴ This one-dimensional character of the stacking differences suggests the description of the differences in terms of an axial next-nearest neighbor Ising (ANNNI) model,¹⁸ where the i th cubic (hexagonal) bilayer is represented by the pseudospin up $\sigma_i \equiv +1$ and down $\sigma_i \equiv -1$. This model has been already successfully applied to the discussion of polytypism of silicon carbide neglecting the contributions of the vibrating lattice.^{19–21} In a simplified version the total free energy of the system per Si-C pair may be represented by

$$F(T) = F_0(T) - \frac{1}{n} \sum_{i=1}^n \sum_{j=1}^{\infty} J_j \sigma_i \sigma_{i+j}, \quad (5)$$

where j runs over the interacting bilayers. The label i accounts for the bilayers in the unit cell of the nH polytype. More complicated interactions, such as four-spin terms, are negligible and therefore have been left out for transparency. The parameters J_j are the interaction energies of two bilayers. The largest term $F_0(T)$ in Eq. (5) represents the energy of the crystal without interaction of the bilayers. Assuming that the long-range interactions are small we restrict the j -sum up to third neighbors ($j=3$).

In order to derive the interaction parameters J_j we replace the total free energy $F(T)$ at a given volume in Eq. (5) by the sum of the lattice contribution and the total internal energy of the electrons.^{3–5} The entropy of the electronic system as well as the configurational contribution, which is related to the arrangement of boundaries between bilayers belonging to different spins, are not taken into account.¹⁷ Explicitly, differences are considered, i.e., $F_{2H} - F_{3C} = 2J_1 + 2J_3$, $F_{4H} - F_{3C} = J_1 + 2J_2 + J_3$, and $F_{6H} - F_{3C} = \frac{2}{3}J_1 + \frac{4}{3}J_2 + 2J_3$. The results of a fitting procedure for the J_i parameters is given in Table I.

The variation of the parameters starting from three different static total energy calculations^{3–5} may be traced back to three facts. (i) The atomic relaxation taken into account by Käckell *et al.*⁴ remarkably reduces the nearest-neighbor interaction J_1 . (ii) The *ab initio* calculation of Cheng *et al.*³ favors the 6H polytype instead of the 4H one. (iii) A much larger energetical difference between 3C and 2H is calculated by Karch *et al.*,⁵ and Cheng *et al.*³ The introduction of the phonon free energy reduces all interaction parameters. We observe a tendency for a reduction of J_1 , J_2 , and J_3 and, respectively, a shift towards more negative values. That means, that the vibrating lattice reduces the attractive character of the nearest-neighbor interactions. Thereby the effect

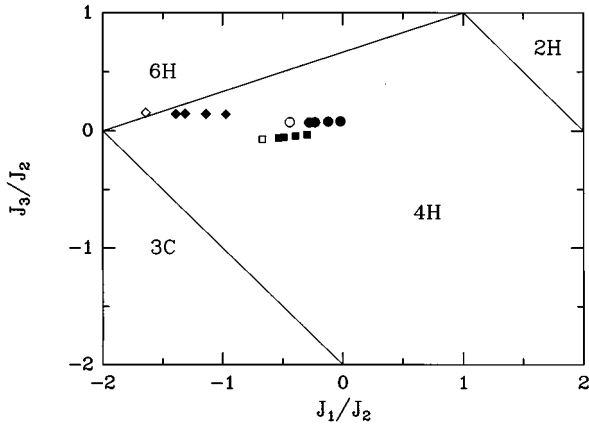


FIG. 4. Phase diagram of the ANNNI model. The stability regions of the four polytypes considered are indicated. The phases obtained starting from the *ab initio* results of Refs. 3–5 are indicated by diamonds, circles, and squares, respectively. Open symbols, without the lattice contribution to the free energy; black symbols, with phonon free energy. From left to right increasing temperatures $T=0$, 400, 800, and 1200 K are considered.

on the second-nearest-neighbor interaction is rather small. The phonon influence on J_1 and J_3 is more important, especially starting from the *ab initio* results of Ref. 5. In this particular case J_3 , i.e., the third-nearest-neighbor interaction will be repulsive for layers of equal pseudospin.

The phase diagram of the described ANNNI model including the phonon contributions is plotted in Fig. 4. We chose the ratios J_3/J_2 and J_1/J_2 as coordinates. In the selected parameter region two multiphase degeneracies appear. For $J_3=0$ and $J_1=-2J_2$ the phases of low hexagonality 3C, 6H, and 4H degenerate. For the more unrealistic parameter configuration $J_1=J_2=J_3$ a triple point of the hexagonal phases under consideration appears. When the lattice contributions to the total free energies are neglected, the results of the three *ab initio* calculations appear close to the first triple point. After inclusion of the lattice free energy the calculated phases appear much more in the stability region of the hexagonal phases. This tendency away from the cubic phase is increased with rising temperature. This result confirms the paradoxical situation²² that SiC appears to prefer to grow in cubic form, more than in any other, in spite of the fact that this is never the stable structure. Surprisingly, we observe a stabilization of the 4H polytype with an increase of the temperature. Although our estimates show also a tendency to increase the ratio J_3/J_2 and thereby to approach the 6H stability region, in the framework of the ANNNI model we cannot reproduce the results of the experiments,^{8,23} which indicate that 6H is the stable form at high temperatures and probably 4H at low temperatures. However, the experimental picture is not completely clear (see Ref. 23).

C. Heat capacity and Debye temperature

The constant volume specific heat $C_V(T)$ of 3C SiC calculated within the framework of BCM and DFT is plotted in Fig. 5(a) versus temperature and compared with available experimental data.²⁴ The BCM data agree very well with the corresponding *ab initio* ones. Moreover, both theoretical ap-

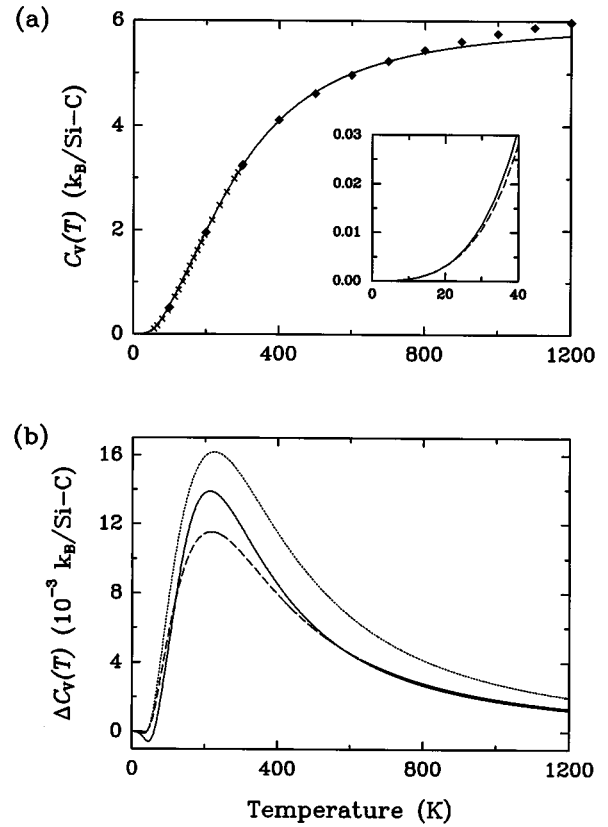


FIG. 5. (a) Specific heat capacity per Si-C pair as a function of temperature calculated within the BC model (solid line) and DFPT (dashed line). The experimental results of the specific heat at constant pressure taken from Ref. 24 are indicated by diamonds and crosses. The inset shows the behavior at low temperatures. (b) Differences of the heat capacity of nH polytype with respect to the 3C value. $C_V^{2H} - C_V^{3C}$ (solid line), $C_V^{4H} - C_V^{3C}$ (dotted line), and $C_V^{6H} - C_V^{3C}$ (dashed line).

proaches reproduce the T^3 law for the low temperature limit and agree with the experimental data in the temperature range between 50 and 800 K excellently. The deviations for higher temperatures are due to the fact that the experimental data were measured at constant pressure. Therefore the anharmonic effects, which become important for high temperatures and are not taken into account in the calculations, cause the differences. The excellent agreement between C_p and C_V below 800 K show on the other hand, that the harmonic approximation provides realistic results in this temperature region. Since the optical phonon frequencies correspond to a temperature of about 1400 K, the Dulong-Petit limit has not been reached inside the plotted temperature interval.

The almost identical course of the specific heat of the different polytypes [see Fig. 5(b)] can be connected with the almost identical free energy of these polytypes [Fig. 2(b)]. This similarity holds especially for very low ($T < 100$ K) and higher temperatures ($T > 600$ K). The largest deviations between the specific heat of the cubic and hexagonal phases of roughly 1% appear at about 200 K.

However, the small variations between the heat capacities of the polytypes considered give rise to different Debye temperatures $\Theta_D(T)$, which were derived from the Debye equation for the specific heat,

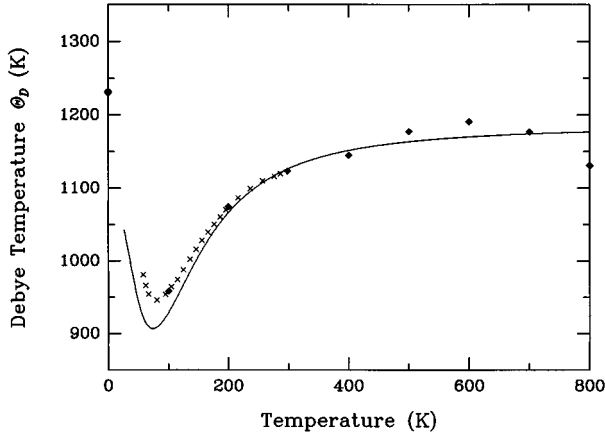


FIG. 6. Debye temperature $\Theta_D(T)$ of 3C SiC. Diamonds and crosses indicate Debye temperatures estimated from experimental specific heat results (Ref. 24). The dot at $T=0$ K denotes a calculated value; see text.

$$C_V(T) = 18k_B \left(\frac{T}{\Theta_D(T)} \right)^3 \int_0^{\Theta_D(T)/T} \frac{x^4 e^x}{(e^x - 1)^2} dx, \quad (6)$$

using a root-finding procedure. The results for 3C SiC are shown in Fig. 6. Similarly to other tetrahedrally coordinated semiconductors, the curve for 3C SiC exhibits a rather strong temperature variation, in particular in the temperature region below room temperature. The agreement with experimental data is reasonable. In the low temperature region around 100 K the theoretical values are somewhat smaller. This could be a consequence of the fact that the sound velocities are slightly underestimated within the BCM.⁷ In Table II we list Debye temperatures calculated at 0 K and 300 K for the considered polytypes of SiC. The differences between the Debye temperatures of cubic SiC and the hexagonal phases at room temperature are rather small. This result agrees well with the experimental data.^{24,25} To get reasonable values for the Debye temperatures around 0 K very dense meshes of \mathbf{q} -points are needed to perform the integration over the Brillouin zone. Therefore we applied another method, which overcomes the high numerical effort for calculating the phonon frequencies at very dense \mathbf{q} -point meshes. In order to calculate the values $\Theta_D(0)$ we determined the mean sound velocity by averaging the gradient of the acoustic branches over a sphere lying very close around the Γ point. We found, in agreement with previous calculations for other materials,²⁶ that the Debye temperature at 0 K lies higher than $\Theta_D(T)$ in the high temperature region. 3C SiC has the largest Debye

TABLE II. Debye temperatures $\Theta_D(T)$ (K) of SiC polytypes derived from the averaged sound velocities for $T=0$ K and expression (6) for 300 K, respectively.

	3C	6H	4H	2H
Theory (0 K)	1232	1205	1211	1208
Theory (300 K)	1126	1123	1120	1122
Expt. (300 K)	1123 ^a	1126 ^b	-	-

^aReference 24.

^bReference 25.

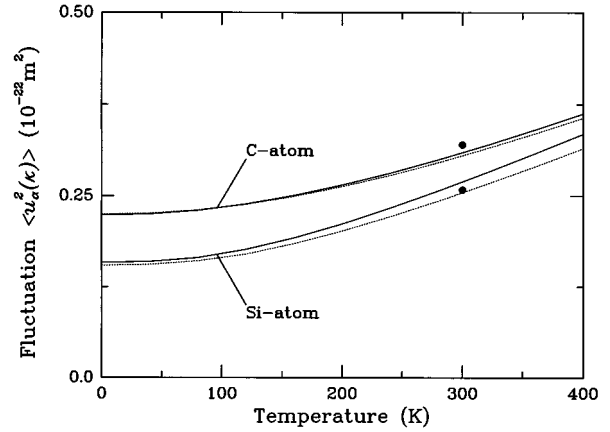


FIG. 7. Mean-square displacement of carbon and silicon atoms of 3C SiC versus temperature. Solid line, BC model; dotted line, DFPT. The averaged values measured for 6H SiC at room temperature are indicated as dots (Ref. 28).

temperature at 0 K, whereas the values for the hexagonal structures are somewhat smaller and among themselves similar in quantity. However, no clear trend with hexagonality, as, e.g., for the band gap or for the Γ point frequencies, is perceptible. 2H and 6H SiC have nearly the same Debye temperatures, while 4H SiC shows a somewhat smaller value. This behavior as a function of the hexagonality follows that of the sound velocities.⁷ The folding of the acoustic branches of 3C along the [111] direction into the hexagonal Brillouin zone causes the flattening of the branches near the zone boundary. In the average, this also gives rise to a lowering of the Debye temperature of the hexagonal phases in comparison with the cubic one. A second reason may be related to the decrease of the zone-center optical frequencies⁷ with hexagonality. When the Debye temperatures are calculated or measured at higher temperatures, the differences between the polytypes vanish, as shown in Table II for room temperature.

D. Displacement-displacement correlations

The most important autocorrelation functions are the vibrational amplitudes of the atomic mean-square displacements. They follow from expression (1) setting $l=l'$, $\kappa=\kappa'$, and $\alpha=\beta$,

$$\langle u_\alpha^2(\kappa l) \rangle = \frac{\hbar}{NM_\kappa} \sum_{\mathbf{q},j} \frac{1}{\omega_j(\mathbf{q})} \left[n(\omega_j(\mathbf{q})) + \frac{1}{2} \right] |e_\alpha^\kappa(j\mathbf{q})|^2. \quad (7)$$

As a consequence of the translational symmetry there is no dependence on the index l of the unit cell in Eq. (7). Figure 7 shows the mean square displacements of the carbon and silicon atoms, the so-called Debye-Waller factors²⁷ for 3C SiC, versus temperature. They are independent of the Cartesian direction α , due to the cubic symmetry of the crystal. The increase with rising temperature indicates the mechanism, which is related to lattice expansion in a real crystal. In the low temperature limit the vibrational amplitude of the lighter carbon atom is larger than that for the silicon atom. In this region, the results obtained within BCM and DFPT agree excellently. This holds also with respect to room-

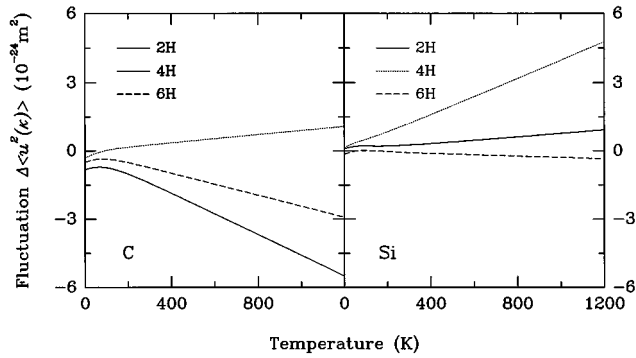


FIG. 8. Fluctuations of the mean square displacements of carbon (left panel) and silicon (right panel) atoms in nH SiC with respect to the $3C$ values. The mean-square displacements are averaged with respect to the inequivalent positions in the unit cell and the Cartesian directions. Solid line, $2H$; dashed line, $4H$; and dotted line, $6H$.

temperature data from x-ray diffraction measurements.²⁸ For room temperature the carbon (silicon) atom is displaced in the average by about 0.057 (0.051) Å from its equilibrium position. For higher temperatures, both curves approach each other. However, this tendency is overestimated within the BCM. We observe even a crossing at about 700 K. In general, the temperature increase is slightly overestimated within the harmonic approximation, because the anharmonic contributions, which lower the values of the phonon frequencies, are not taken into account. The deviations between results of BCM and DFPT are larger than in the case of free energy or heat capacity. This is due to the need of the eigenvectors in the computation of the autocorrelation functions [see Eq. (7)]. Actually we have found that in the case of $3C$ SiC the agreement of the eigenvectors from BCM and DFPT (Ref. 7) is excellent along the high-symmetry directions ΓX and ΓL in the BZ. Nevertheless, there are small deviations, especially in low-symmetry directions. These small deviations become important for higher temperatures and acoustic modes because of the weighting factor $[\omega_j(\mathbf{q})]^{-2}$ of the square of the eigenvectors.

Because of the sensitivity of the displacement-displacement correlation to the exact values of the eigenvectors and eigenfrequencies, we only compute deviations of the mean square displacements in the hexagonal polytypes $6H$, $4H$, and $2H$ with respect to the $3C$ values within the BCM. First, we consider the mean square displacements averaged over the different space directions and the geometrically inequivalent atoms.

In order to represent the influence of polytypism on the Debye-Waller factors we show in Fig. 8 the differences of the mean square displacements for the different carbon and silicon atoms in the nH unit cell with respect to the zincblende values. We observe a similar dependence on the polytypes as found for the free energy, entropy, and Debye temperature. The results for the $4H$ polytype are quite different compared to those of $2H$ and $6H$ considering thermal properties. Whereas in the case of silicon atoms the averaged displacements of $2H$, $6H$, and $3C$ are nearly the same, the averaged silicon displacements in $4H$ seem to be always larger than in the other polytypes. Moreover, the averaged

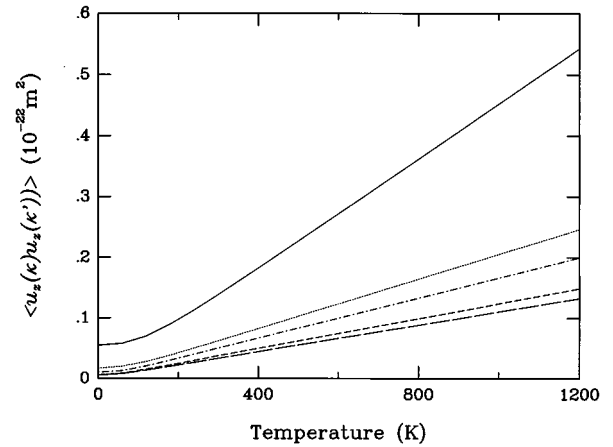


FIG. 9. The z - z -displacement correlation function of the first- (solid line), second- (dotted line), third- (short dashed line), fourth- (long dashed line), and fifth-nearest (dot dashed line) neighbor atoms in $3C$ SiC.

mean-square displacements of the carbon atoms are smaller in $6H$ and $2H$, but larger in $4H$. Considering the mean square displacements, we can therefore suppose that the Si-C lattice of $4H$ should be more expanded with temperature than those of $3C$, $6H$, and $2H$ SiC.

We have also examined the deviations of the mean-square displacements for the $n/2$ inequivalent C and Si atoms in the nH unit cell and the inequivalent displacement directions parallel and perpendicular to the c axis from the $3C$ values. However, these deviations are of the order of 1% compared to the averaged values, indicating a rather small anisotropy and almost vanishing inequivalence of the atoms in the hexagonal nH structures. These findings are somewhat in contrast to x-ray measurements for $6H$ SiC,²⁸ which seem to be only explainable with fluctuations between the inequivalent atoms that are one order of magnitude larger.

The displacement-displacement correlation functions of different atoms are much smaller (by about a factor 10) than the autocorrelation functions. As an example, the functions $\langle u_z(\kappa)u_z(\kappa') \rangle$ up to fifth nearest neighbor atoms $\kappa' = 1, \dots, 5$ with respect to a carbon atom $\kappa = 0$ situated at the origin of coordinates are plotted in Fig. 9 for $3C$ SiC versus temperature. The calculation has been performed within a hexagonal unit cell. It is known that besides the first- and second-nearest-neighbor interaction, the interaction along the zigzag chains in cubic $[110]$ directions, including the origin and the fifth neighbor atom, is the most important one. This has been already shown for silicon.²⁹ This expectation is also confirmed for $3C$ SiC, as can be seen from Fig. 9. The correlations between atoms 0 and 5 are stronger than those between 0 and 3 or 0 and 4, because these atoms are not in the plane containing the Si-C zigzag chain. Always three (four) bonds are needed to reach the atom 3 or 5 (4), starting from atom 0. However, only in the case of the 0-5 correlation are all these bonds arranged in one plane. Equivalent calculations for the hexagonal polytypes have yielded similar results, but no trend with the hexagonality could be observed. Moreover, also in the case of $2H$ SiC the correlations of neighboring atoms are practically identical with

those of 3C SiC. This is somewhat surprising since atom 5 belongs in the wurtzite structure to a twisted bilayer of atoms.

IV. SUMMARY

We have presented calculations of thermal properties of cubic and hexagonal silicon carbide polytypes using a generalized bond-charge model which describes the underlying lattice dynamics. More in detail, thermodynamical functions such as free energy and entropy as well as heat capacity and displacement-displacement correlations have been considered. In order to check the reliability of the model calculations, we have compared all results for the zinc-blende polytype 3C SiC with those obtained within an *ab initio* density-functional method, where the response of the system to atomic displacements and external fields is self-consistently calculated. The studies of the thermodynamics of the polytypes has been completed with an ANNNI model using temperature-dependent coefficients. This model allows the discussion of the phase equilibrium of the polytypes 3C, 6H, 4H, and 2H and of tendencies for stabilization of different polytypes in dependence on temperature. The calculated heat capacity at constant volume is in excellent agree-

ment with experiment. The Debye temperatures derived from the specific heat give only a weakly pronounced trend with the percentage hexagonality at very low temperatures. Moreover, the differences of the Debye temperatures of the *nH* SiC polytypes decrease rapidly with increasing temperature. This fact agrees well with experimental findings for 3C and 6H SiC. The mean square displacements are very interesting in the context of x-ray or neutron scattering, where they enter the Debye-Waller factor. Their absolute values agree well with room temperature experimental data. We find a relatively small variation of the mean-square displacement with respect to the geometrically inequivalent atoms in the hexagonal unit cell. The same holds for the anisotropy of the vibrational amplitudes. In general, these variations are rather small due to the small anisotropy of the hexagonal polytypes of SiC under normal conditions.

ACKNOWLEDGMENT

This work has been supported by the Deutsche Forschungsgemeinschaft (Sonderforschungsbereich 196, project A8). A part of the numerical calculations has been done on the Cray-YMP of the KFA in Jülich and the Leibniz-Rechenzentrum in München.

-
- ¹N. W. Jepps and T. Page, in *Progress in Crystal Growth and Characterization*, edited by P. Krishna (Pergamon, Oxford, 1983), Vol. 7, p. 259.
- ²A. Verma and P. Krishna, *Polymorphism and Polytypism in Crystals* (Wiley, New York, 1966).
- ³C. Cheng, V. Heine, and R. J. Needs, *J. Phys. Condens. Matter* **2**, 5115 (1990).
- ⁴P. Käckell, B. Wenzien, and F. Bechstedt, *Phys. Rev. B* **50**, 10 761 (1994).
- ⁵K. Karch, G. Wellenhofer, P. Pavone, U. Rössler, and D. Strauch, in *Proceedings of the 22nd International Conference on the Physics of Semiconductors, Vancouver, 1994*, edited by D.J. Lockwood (World Scientific, Singapore, 1995), p. 401.
- ⁶*Numerical Data and Functional Relationships in Science and Technology*, edited by O. Madelung, Landolt-Börnstein, New Series, Group III, Vols. 17a and 22a (Springer, Berlin, 1982 and 1986).
- ⁷M. Hofmann, A. Zywiets, K. Karch, and F. Bechstedt, *Phys. Rev. B* **50**, 13 401 (1994).
- ⁸D. Pandey, *Phase Trans.* **16/17**, 247 (1989).
- ⁹K. Karch, P. Pavone, W. Windl, D. Strauch, and F. Bechstedt, *Int. J. Quantum Chem.* **56**, 801 (1995).
- ¹⁰K. Karch, P. Pavone, A. P. Mayer, F. Bechstedt, and D. Strauch, *Physica B* (to be published).
- ¹¹D. C. Wallace, *Thermodynamics of Crystals* (Wiley, New York, 1972).
- ¹²P. C. Trivedi, *J. Phys. C* **18**, 983 (1985).
- ¹³K. Karch, T. Dietrich, W. Windl, P. Pavone, A. P. Mayer, and D. Strauch, *Phys. Rev. B* **53**, 7259 (1996).
- ¹⁴K. Karch and F. Bechstedt (unpublished).
- ¹⁵R. W. G. Wyckhoff, *Crystal Structures* (Interscience Publishers, New York, 1964), Vol. 1.
- ¹⁶H. J. Monkhorst and J. K. Pack, *Phys. Rev. B* **13**, 5188 (1976).
- ¹⁷C. Cheng, V. Heine, and I. L. Jones, *J. Phys. Condens. Matter* **2**, 5097 (1990).
- ¹⁸J. von Boehm and P. Bak, *Phys. Rev. Lett.* **42**, 122 (1979).
- ¹⁹C. Cheng, R. J. Needs, V. Heine, and N. Churcher, *Europhys. Lett.* **3**, 475 (1987).
- ²⁰C. Cheng, R. J. Needs, and V. Heine, *J. Phys. Solid State Phys.* **21**, 1049 (1988).
- ²¹J. J. A. Shaw and V. Heine, *J. Phys. Condens. Matter* **2**, 4351 (1990).
- ²²V. Heine, C. Cheng, and R. J. Needs, *J. Am. Ceram. Soc.* **74**, 2630 (1991).
- ²³N. W. Jepps and T. F. Page, *Prog. Cryst. Growth Charact.* **7**, 259 (1983).
- ²⁴L. V. Gurvich and I. V. Veyts, *Thermodynamic Properties of Individual Substances* (Hemisphere Publishing Corporation, New York, 1972).
- ²⁵D. R. Stull and H. Prophet, *JANAF Thermochemical Tables*, Nat. Stand. Ref. Data Ser., Nat. Bur. Stand. (U.S.) (Washington, D.C., 1971), p. 37.
- ²⁶G. Nilsson and S. Rolandson, *Phys. Rev. B* **7**, 2393 (1971).
- ²⁷N. W. Ashcroft and N. D. Mermin, *Solid State Physics* (Saunders College, Philadelphia 1976).
- ²⁸A. Bram, Diploma thesis, Universität Erlangen-Nürnberg, Erlangen, 1990.
- ²⁹A. Mazur and J. Pollmann, *Phys. Rev. B* **39**, 5261 (1989).